THE ASTROPHYSICAL JOURNAL, 405:153–162, 1993 March 1

AN H I ABSORPTION SURVEY OF M31 AND M33: THE MIXTURE OF WARM AND COOL PHASES IN THE INTERSTELLAR MEDIA OF SPIRAL GALAXIES

JOHN M. DICKEY
Department of Astronomy, University of Minnesota, 116 Church Street S.E., Minneapolis, MN 55455
AND
ELIAS BRINKS
National Radio Astronomy Observatory, P.O. Box O, Socorro, NM 87801
Received 1992 July 20; accepted 1992 September 8

ABSTRACT

We have used the VLA in A-array to survey the nearby spiral galaxies M31 and M33 in the 21 cm line to measure absorption by their H I toward background continuum sources. After a total of more than 30 hr of integration, we have obtained spectral line cubes with rms noise less than 1.2 mJy in spectral channels of 2.6 km s^{-1}. With our clean beam size of 5″ (16 pc), we see no emission from M31 and very little emission from M33. In M31 there are 11 continuum sources in our field of view that are stronger than 5 mJy toward which we can measure absorption spectra; in M33 there are 10. Of these, five show absorption in the 21 cm line, and the rest do not. Comparing with emission surveys done with the Westerbork Synthesis Radio Telescope, we can determine the mixture of warm and cool atomic gas on each line of sight.

Our major result is that the warm neutral medium is the dominant form of atomic hydrogen in M31 and M33, as it is in the Milky Way. Clearly this phase is robust to variations in the interstellar environment represented by the differences among these galaxies. Compared with the Milky Way, M31 shows somewhat more cool atomic hydrogen (40% relative to 25%), whereas M33 shows less (15%). This suggests a trend with morphological type, with Sb galaxies showing more cool H I relative to warm, and Sc galaxies less, a trend similar to that seen by comparing molecular with atomic gas overall.

Our results are in agreement with the findings of Braun & Walterbos (1992) for a different field in M31. We differ in our interpretation of the peak 21 cm brightness temperature and its relationship to the average absorption coefficient, $\langle\kappa\rangle$, measured by our absorption surveys. In the Milky Way, $\langle\kappa\rangle$ determines the brightness temperature at which the emission saturates. In M31, because of its high inclination and because of the vertical stratification of the warm and cool gas, the peak surface brightness of the 21 cm emission is much higher than what we see in the Milky Way. In M33 the emission is not saturated, because the inclination is low enough so that the covering factor of optically thick clouds is very small. Thus the differences in the average 21 cm absorption coefficient among the three galaxies, combined with our different vantage points, explains the differences in their emission properties without the need to invoke different spin temperatures for the cool phase gas in the different galaxies.

Subject headings: galaxies: individual (M31, M33) — galaxies: ISM — radio lines: ISM

1. INTRODUCTION

The interstellar gas in the Milky Way is mostly found in one of several distinct "phases," with characteristic values of density and temperature, which we label with names like "hot," "warm ionized," "warm neutral," "cool atomic," and "molecular," among others (see the review by Kulkarni & Heiles 1987). The relative abundances of the different phases are determined by the energy flow through the medium. This is true both for static equilibrium models such as that of Field, Goldsmith, & Habing (1969) and dynamic models following the paradigm of McKee & Ostriker (1977). In the former, the gas pressure determines which phases can be in heating and cooling equilibrium; a relatively narrow range of pressures allows both warm and cool atomic gas phases to coexist. In dynamic models the pressure is not constant but fluctuates randomly with time at each point, with a distribution which depends on the supernova rate. The exchange of material among the diffuse cool clouds, the hot ionized medium, and the warm media (neutral and ionized) depends critically on this "pressure spectrum," and on other physical parameters such as the magnetic field strength, the heavy-element abundance, and the spatial clustering of the supernovae (Wang & Cowie 1988; Heiles 1990). The astrophysical question of how robust is the mixture of phases which we find locally in the Milky Way against changes in these quantities can be addressed by observing nearby spirals to see whether they have different relative abundances of gas in the various phases. A first attempt to do just this was made by us for a field close to the center of M31 (Dickey & Brinks 1988, hereafter DB). We used the VLA[1] in its B-configuration and looked for 21 cm absorption against six sources. Apparently the warm neutral medium is robust, since we find about the same fraction (25%) of atomic hydrogen in the cool phase as in the solar neighborhood. Braun & Walterbos (1992), analyzing the VLA survey of the northern half of M31, discuss absorption against another seven sources. They find several absorption lines, with more absorption on average than was found by DB. In this project we report on more sensitive and higher velocity resolution VLA observations on

[1] The VLA is part of the National Radio Astronomy Observatory, which is operated by Associated Universities, Inc., under cooperative agreement with the National Science Foundation.

another field in M31, adding 11 more lines of sight, in order to measure the fraction of atomic gas which is in the cool phase. In addition, we report on a deep integration of a field in M33, hoping to see variation, if any, with Hubble type in the structure of the interstellar medium (ISM).

In the Milky Way about 25% of the H I is in the cool phase and 75% in the warm phase. In the inner galaxy this ratio appears to change, but how much and in what sense is still a matter of discussion (Garwood & Dickey 1988; Frail et al. 1991; Kobulnicky, Dickey, & Garwood 1993). The Milky Way may be extraordinary in having just the right conditions to allow both warm and cool atomic phases to exist, or it may be that most spiral galaxies somehow achieve this state, perhaps by some self-regulating process which keeps the pressure in the right range. This is important for the question of cloud formation, since the transition between the warm and cool neutral phases is where the medium goes from a widespread, diffuse, "intercloud" state, with a high spatial filling factor, into more or less discrete structures with much lower filling factor, which we describe loosely as clouds. These clouds ultimately become the raw material for star formation and so determine the evolution of the galaxy as a whole (Shaya & Federman 1987; Wyse 1986).

Just as the transition between warm and cool atomic phases represents the transition from intercloud to cloud material, the atomic gas as a whole constitutes an intermediate state between the hot, ionized gas which fills most of the halo and much of the disk of a spiral like the Milky Way, and the molecular clouds, which have a tiny filling factor but contain most of the mass of interstellar gas. In some spiral galaxies cloud formation is so efficient that all the gas is gathered into molecular clouds, with atomic gas present only as the product of photodissociation of molecules by radiation from young stars (e.g., M51; Tilanus & Allen 1989). This may even be typical of the inner disk of the Milky Way. It is also common to see a fountain or wind of ionized gas driven out of the disk, presumably by the high pressure generated by a high supernova rate (Norman & Ikeuchi 1989; Cox 1990; Rand, Kulkarni, & Hester 1990; Hunter & Gallagher 1990; Cox & McCammon 1986). Somehow most spiral galaxies avoid the extremes of either a fully ionized or a fully molecular interstellar medium, or an interstellar medium with only star-forming molecular clouds plus a hot ionized wind from the resulting supernova remnants, since we generally find that the atomic gas is a significant fraction of the interstellar gas mass even in the inner, star-forming disk of most galaxies.

Of all the interstellar phases, the least robust is the warm neutral medium, since it is most vulnerable either to condensation onto clouds or to heating and ionization by supernova remnants (Cowie 1987). In the Milky Way the high abundance of warm neutral medium relative to cool neutral medium is a particularly difficult quantity to explain theoretically (reviewed by Kulkarni & Heiles 1988). Observationally, these two can be separated most directly by comparing emission and absorption in the 21 cm line (reviewed by Dickey & Lockman 1990); in fact, it was such observations which first motivated multiphase theories of the interstellar gas (Clark 1965). It is now possible to extend such emission/absorption studies of the 21 cm line to other galaxies to see whether the warm neutral medium is a significant fraction of the atomic gas in other environments.

Absorption in the 21 cm line arises exclusively in the cool gas, because the absorption coefficient κ is inversely proportional to temperature. The emission coefficient is independent of temperature, so that the 21 cm brightness temperature measures column density per unit velocity interval, unless the gas is optically thick. By measuring absorption spectra through spiral disks, we measure the line-of-sight integral of density divided by temperature; comparing this with the column density measured in emission gives the mean temperature, as described below (§ 3).

Section 2 describes the observational techniques. Section 3 presents the spectra and explains the computation of the fractions of atomic gas in the warm and cool phases. Section 4 discusses the results in terms of the differences among the Milky Way, M31, and M33 in their cool gas fractions. As discussed in § 4 also, this contrast helps us understand other differences among these three galaxies, such as their peak 21 cm brightness temperatures. This issue turns on the question of how the warm and cool phases are distributed in z, i.e., height above the plane. Since the mixture of atomic phases is particularly sensitive to pressure, other spiral galaxies probably have vertical stratification of temperature similar to that seen in the solar neighborhood, although this question is still controversial.

2. OBSERVATIONS

In order to measure 21 cm absorption, it is necessary to eliminate the emission. That can be done most directly by using an interferometer with fringe separation finer than the spatial variations in brightness of the emission. If emission and absorption are mixed in the data, it is possible to interpolate from around the background source and subtract the emission in front of the source, in order to isolate the absorption, but this is difficult in practice (Dickey, Brinks, & Puche 1992). For other galaxies, even as close as M31 and M33, the A-array of the VLA is needed to resolve away the emission. In the long term it would be nice to have maps of the 21 cm emission and absorption with all spatial scales combined (single dish plus all VLA spacings), but in practice it would take a huge amount of integration time in the A-array to detect and map the small-scale structure of the 21 cm emission. Even with 12 hr of integration on M31, we see no trace of emission in our A-array data; with 18 hr of integration on M33 we see emission only statistically through a slight increase in the fluctuations of brightness at the velocity of the galaxy. The continuum background sources, being mostly extragalactic (i.e., far behind M31 and M33), are quite small in angular size. With some tapering, the A-array detects most of their continuum flux, so the absorption spectra come through cleanly without pollution by emission.

Absorption lines, because they arise from cool gas, have line widths of only a few kilometers per second. Observing with spectral resolution more than 2 or 3 km s^{-1} underresolves the lines in frequency and causes their optical depth to be underestimated. To be sensitive to such narrow lines over the entire velocity range of a galaxy requires at least 250 spectral channels, sometimes more. Meanwhile, since receivers are radiometer-noise–limited, these narrow channel bandwidths cause the sensitivity to be a limiting factor. Even with the VLA, it takes $\sim$10 hr integration time to be able to detect a line of optical depth 1 (attenuation by 63%) in a 1.5 km s^{-1} channel toward a 10 mJy continuum source. Finally, although there are enough such continuum background sources to sample many lines of sight through a nearby galaxy, they are distributed at random. To cover many of them requires either many consecu-

tive long integrations, or, with an aperture synthesis telescope, it requires that the entire primary beam area be mapped. So an experiment like this presents a massive data processing burden.

The data were taken during a 48 hr session on 1989 February 8–11. We recorded 351 baselines times 2 polarizations times 128 channels with averaging time on-line of 20 s. The short averaging time was necessary to reduce the attenuation and distortion of sources far from the phase center. The on-line Hanning smoothing option was used, so that the final channels have only 10% overlap. Specific parameters of the observation and data reduction are given in Table 1. We chose a field in M31 located to the southwest of the nucleus centered in such a way as to maximize the number of background sources within the primary beam. We used the Westerbork Synthesis Radio Telescope (WSRT) 20 cm continuum survey of Walterbos, Brinks, & Shane (1985) to guide us. This field was expected to add about a dozen new lines of sight to the ones already published by DB and BW. The selection of the field in M33 was based on the WSRT survey published by Viallefond et al. (1986).

The data were edited and calibrated using the AIPS (1991 July 15) routines. The bandpass calibration was particularly crucial for this experiment; by using the strong source 1328+307 as a bandpass calibrator, we achieve a very flat bandpass, with ripples less than a few times 10^{-3} in gain. On the extreme edges we have dropped a total of 16 channels because of IF filter attenuation.

We experimented with many methods for mapping; the most efficient technique was to use the task HORUS after applying the calibration using SPLIT. We used natural weighting for optimum sensitivity; this makes almost a factor of 2 difference in the rms noise compared with the default, uniform weighting. In order to exclude all traces of the extended emission, we set an absolute lower *uv* limit of 1 km, which means that there is nothing in our maps with scales larger than about 30″ or 100 pc. In order to get the most flux from the partially resolved continuum sources, we taper the *uv* data; the Gaussian tapering function has half-width 60 kλ, although our maximum baseline is about 180 kλ. This taper increases the noise by less than 50%, and it has the added advantage of allowing us to map with larger pixels. In order not to miss any background sources, we first made continuum maps with 2048 × 2048 pixels to find the sources. In making the cube, we then shift the center so that all useful continuum sources are included. Our final 1024 × 1024 maps cover almost the entire primary-beam area. Even though our beam size after tapering comes out similar to that of the B-array, the distribution of baselines is of course quite different. Because of the centrally condensed nature of the VLA *uv* coverage, our 1 km lower *uv* limit would have excluded much more data from a B-array observation. Thus it was necessary for this experiment to use the A-array in spite of the increased computational difficulties.

The final synthesized beam size of 5″ corresponds to 16 pc at the nominal M31 distance of 690 kpc (or 17 pc at the nominal distance of 720 kpc to M33); the total area of our Gaussian clean beam corresponds to 342 pc^2. Our spectral line noise level (1 σ) of 1.16 mJy beam^{-1} corresponds to ~25 K of brightness temperature. This intensity in a single 2.58 km s^{-1} channel translates to column density $N_H = 1.2 \times 10^{20}$ cm^{-2}. At M31's distance this column density filling our beam would require a total atomic hydrogen mass of 320 $M_\odot$. We see essentially no trace of 21 cm emission in our cubes of M31. A slight indication of widespread emission fluctuations is present in M33, but this is only detectable statistically over a large area. In any given beam area the emission is well below the noise level.

TABLE 1

OBSERVATIONAL PARAMETERS

Parameter	M31	M33
Phase and pointing center:		
R.A. (1950)	$00^h37^m36^s.0$	$01^h31^m25^s.0$
Decl. (1950)	+40°45′00″	+30°42′00″
Total integration time	12^h × 2 IFs	18^h × 2 IFs
Calibration sources:		
Phase and gain	0026+346	0133+476
Flux and bandpass	1328+307	1328±307
Center velocity ($cz_{\rm heliocentric}$)	−450 km s^{-1}	−200 km s^{-1}
Useful velocity range	$-309 > v > -596$ km s^{-1}	$-59 > v > -346$ km s^{-1}
rms noise in cubes	1.16 mJy beam^{-1}	1.17 mJy beam^{-1}
rms noise in continuum maps	220 μJy beam^{-1}	185 μJy beam^{-1}
Pixel size	2″.1	1″.7
Cube center:		
R.A. (1950)	$00^h37^m31^s.159$	$01^h31^m31^s.59$
Decl. (1950)	40°46′07″.894	30°42′42″.29
Clean beam size	5″.7 × 4″.9 (p.a. = 72°), Ω_b = 32 arcsec^2	6″.6 × 5″.5 (p.a. = 60°), Ω_b = 42 arcsec^2
Brightness conversion	1 mJy beam^{-1} = 21.7 K	1 mJy beam^{-1} = 16.5 K
Primary beam size	FWHM = 32′	
Average time	20 s	
Spectrometer bandwidth	1.5625 MHz = 330.3 km s^{-1}	
Channel spacing	δv = 2.57 km s^{-1} (after Hanning smoothing)	
Polarizations	2 (RCP + LCP, mode 2AD-H)	
Number of antennas	25	
Array configuration	A	
Minimum *uv* cutoff	4.74 × 10^3 λ (1 km)	
uv taper	6 × 10^4 λ (12.7)	
uv weighting	Natural	

TABLE 2

CONTINUUM SOURCES AND ABSORPTION SENSITIVITY

A. M31

37W[a] (1)	R.A. (1950) (2)	Decl. (1950) (3)	S_{max} (mJy) (4)	σ_τ (5)	N_H (10^{19} cm^{-2}) (6)	$T_{B\,max}$ (K) (7)
021	$00^h36^m05^s.12$	+40°59′39″.7	47.4	0.13	...	...
027	36 34.60	46 31.2	7.7	0.30	18	5.0
043	37 05.97	47 52.8	9.5	0.20	38	11.1
045	37 12.03	55 04.6	10.2	0.16	20	7.1
050	37 30.15	52 08.8	16.7	0.10	65	11.2
051	37 30.30	33 37.2	21.9	0.13	134	15.9
052	37 33.40	41 57.0	13.3	0.12	136	15.3
057	37 40.74	50 45.5	17.1	0.10	86	18.7
067	38 12.25	40 56.3	24.9	0.06	152	27.9
081	38 35.93	54 16.2	13.1	0.21	295	31.6
091	38 57.34	47 08.2	31.2	0.15	28	8.7

B. M33

V[a] (1)	R.A. (1950) (2)	Decl. (1950) (3)	S_{max} (mJy) (4)	σ_τ (5)	N_H (10^{19} cm^{-2}) (6)	$T_{B\,max}$ (K) (7)
V2	$01^h29^m33^s.64$	+30°28′43″.1	99.0	0.16	<50	2.1
V8	30 36.89	34 45.4	2.8	0.25	134	31.9
V11	30 40.05	30 15.1	22.3	0.12	117	14.4
V27	31 25.11	38 50.8	7.3	0.16	77	14.9
V32	31 39.92	47 48.7	8.0	0.09	87	19.8
V33	31 40.93	35 41.8	2.9	0.18	41	3.9
V37	32 18.30	50 10.5	13.8	0.13	47	12.3
V38	32 23.59	55 12.7	34.1	0.11	<50	2.2
V39	32 26.28	39 35.4	5.1	0.16	69	12.6
V106 = NGC 604	31 42.57	31 39.2	4.2	0.23	238	32.7

[a] See text.

The continuum sources toward which we have searched for absorption are presented in Table 2. The columns of Table 2 list the source name (in the notation of Walterbos et al. 1985 for M31 and Viallefond et al. 1986 for M33), the position, the peak continuum flux, the noise level in the optical depth spectrum, the total column density of H I emission, and the peak brightness temperature of the emission. The positions and peak intensities of the continuum sources were determined using the AIPS verb MAXFIT. Fluxes are peak values as measured by our beam corrected for attenuation by the primary-beam pattern. In most cases these peak fluxes are somewhat less than the integrated flux of the source (i.e., including extended continuum emission).

For M31 the H I emission data for the directions of the continuum sources comes from the WSRT survey of Brinks & Shane (1984); for M33 we use the WSRT survey of Deul & van der Hulst (1987). The column densities are direct integrals of the emission spectra over velocity, converted using

$$N = \int T_B(v)dv \times 1.82 \times 10^{18}\ \mathrm{cm}^{-2}\ (\mathrm{K\ km\ s}^{-1})^{-1}\ .$$

The first source in M31 (37W021) is outside the area mapped by the WSRT; the emission is probably less than 1 K in that area. Channels in the M31 emission cube have been blanked in areas where the emission is less than about 3 K. The M31 emission data correspond to the single-pixel spectra closest to each background source. Since the WSRT beam in this case was 24″ × 36″ (Ω_{beam} = 976 arcsec^2), a typical continuum source of 10 mJy gives only about 7 K of brightness temperature, so even a deep absorption line would have little effect on the emission, which is often 30–40 K at the peak. In M33 we average an area of 45″ × 45″ centered on the background source to generate the emission spectra, in order to improve the signal-to-noise ratio.

Ultimately it would be good to obtain high-resolution maps of the emission to make a more precise matching of emission and absorption in each small region in front of a continuum background source. The combined B-, C-, and D-array maps of a different field in M31 by Braun (1990a, b) are a good example of what is possible with the VLA. Even with such maps in hand, however, it is necessary to interpolate the emission over the area of the continuum source, since it is impossible (except in Galactic studies using pulsar background sources) to measure the emission and absorption both in the same beam area. At the distance of M31 the WSRT beam is 80 pc × 120 pc, whereas our tapered A-array beam is 16 pc × 19 pc. Since this is roughly the area subtended by one of the background sources, interpolation over an area larger than the typical small-scale structure of the hydrogen (<5 pc) is inevitable in any case. For comparison, high-latitude surveys of H I absorption in the Milky Way study gas at about 200 pc distance. At that distance the Arecibo beam size of 3′ (0.2 pc) is small enough to do the interpolation reliably, whereas the 10′ (0.7 pc) beam size of 100 m class telescopes is not (e.g., Payne, Salpeter, & Terzian 1983 and references therein). Thus, in M31, for any individual background source it is dangerous to match

the absorption with the interpolated emission spectrum channel for channel to derive a temperature versus velocity profile, since the errors introduced in any given channel of the emission spectrum by the interpolation are too large. So even if we had a complete synthesis of the emission with all possible array spacings, it would still be impossible to measure precise spin temperatures of individual spectral channels. In the analysis below we concentrate instead on a statistical comparison of the integrals of the emission and absorption spectra to get the average thermal properties of the interstellar hydrogen in the different galaxies.

3. RESULTS

Surveys of absorption toward extragalactic background sources chosen simply for their continuum flux density and small size always have the fundamental problem that the sources are in the wrong places. Particularly interesting, gas-rich regions seldom have any continuum sources behind, and, if they have any, they are usually weak ones. The noise level in absorption (σ_τ in Table 2, col. [5]) is inversely proportional to the continuum flux of the background source, so characteristically the most interesting spectra are among the noisiest. This is particularly a problem for this experiment, as our channel width is so narrow that the noise in even our best absorption spectra is fairly high in spite of our relatively long integration times.

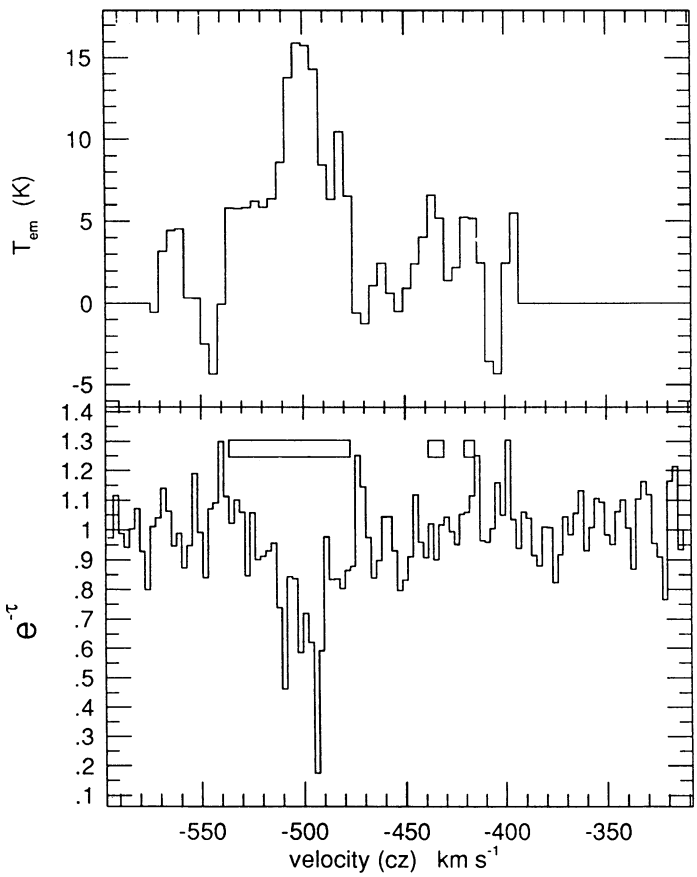

FIG. 1.—Spectra toward 37W051 in M31. The lower panel shows the absorption spectrum, with the emission above. The velocity scale (in km s^{-1}) is at the bottom, and the fractional absorption ($e^{-\tau}$) and the emission brightness temperature (in K) scales are on the left axis. The boxes indicate the velocity ranges used for the integrals on Table 3. The emission cube has been blanked at velocities far from the H I emission, which explains the flat baselines at the edges.

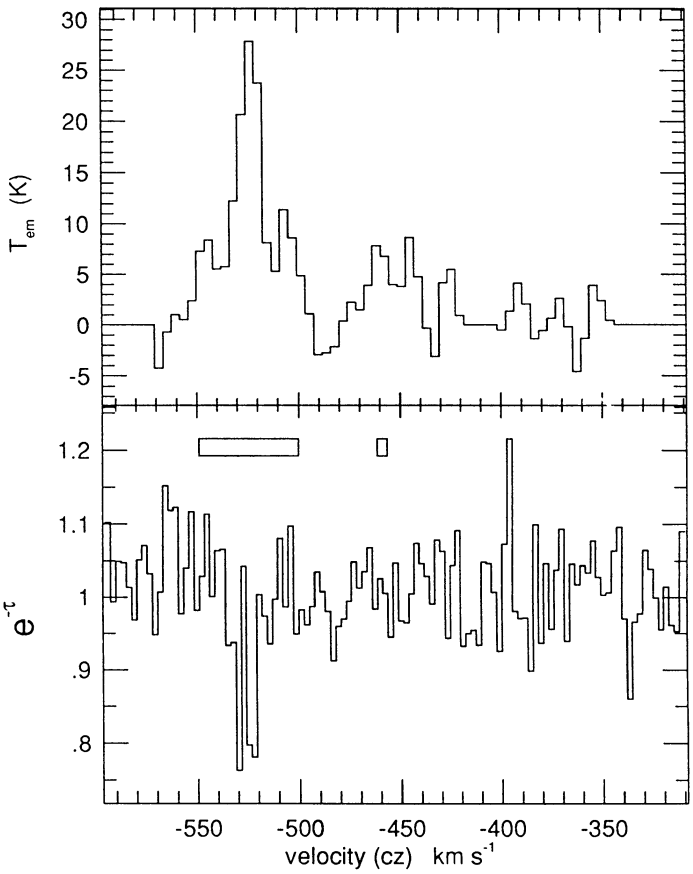

FIG. 2.—Spectra toward 37W067 in M31, presented as in Fig. 1

Spectra showing absorption or tentative absorption lines are shown in Figures 1–5. In many cases the absorption lines are in the 2 σ to 3 σ range, where σ is the noise in the absorption spectrum, computed over velocities where there is no emission. Sensitivity is a severe problem for comparing emission and absorption in individual channels. Typically the peak emission brightness temperatures in Table 2, column (7), are roughly 100 times the rms noise in absorption, so that the gas would have to be cooler than 50 K in order to show absorption above a threshold of even 2 σ [i.e., $T_{sp} < T_B/(2\sigma_\tau)$]. This is the case toward 37W051 and 37W067 in M31 and toward V11 in M33, where the nominal spin temperature [$T_{sp} \equiv T_B/(1 - e^{-\tau})$] is in the range 20–50 K. Although there are not many deep lines detected, the presence of significant absorption in even these few cases shows that cool H I gas is common in the disk of M31 and at least sometimes present in M33.

Many of the spectra which do not show detected absorption in individual channels contain clear indications of absorption at lower levels spread over the velocity range of the emission. A good example is the direction toward 37W081 (Fig. 3). This line of sight passes through a gas-rich region of M31, with emission brightness temperature as high as 32 K, and emission integral $N_H = 3 \times 10^{21}$ atoms cm^{-2}. Although the background source is faint in the continuum (13.1 mJy), and therefore the noise in the absorption spectrum is high, there is clear evidence for absorption seen by comparing statistically the

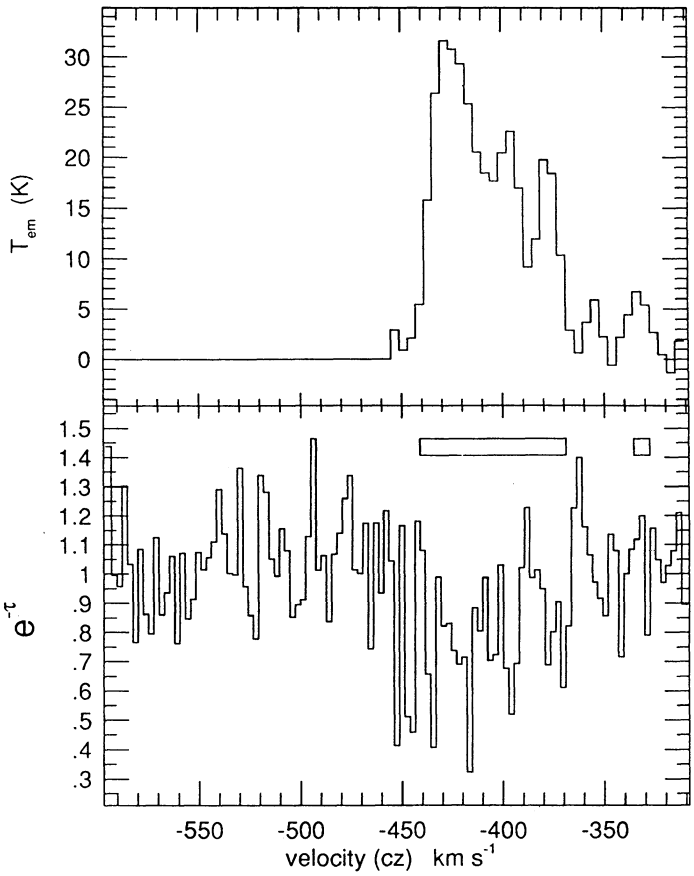

FIG. 3.—Spectra toward 37W081 in M31, presented as in Fig. 1

channels in the absorption spectrum at velocities where the emission is strong with the channels well away from the emission. Comparing integrals of emission and absorption spectra from the same regions is more appropriate than matching channel for channel to compute spin temperatures for each channel, both because of the noise in the spectra and because of the difference in beam sizes between absorption and emission as discussed in § 2.

Since we have high-quality emission spectra, albeit with somewhat larger beam size than for the absorption, we know a priori what velocity range to integrate in search of broad absorption below the single-channel detection threshold. In computing these integrals, we include only absorption channels for which the corresponding emission brightness is above 5 K. Channels outside this range are used to fit the level of the baseline. The velocity ranges selected in this way are indicated in Figures 1–5 by the rectangles above the absorption spectra.

The result of the spectral integration is shown in Table 3. Column (1) lists the source name as in Table 2. Column (2) gives the integral of $(1 - e^{-\tau})$ over those channels of the absorption spectrum corresponding to velocities where the emission T_B is above the threshold of 5 K. Column (3) gives the integral of the emission over the same velocity range (note that these values are smaller than the integrals in Table 2, col. [6], which cover all velocities). Column (4) gives the velocity width covered by the preceding integrals. Using this velocity width and the rms in the absorption spectra from Table 2, we get the ($\pm 1\ \sigma$) error bars for the optical depth integral given in column (2). Column (5) gives either 3 σ lower limits or $\pm 1\ \sigma$ ranges for the mean spin temperature resulting from dividing column (3) by column (2).

The mean spin temperature $\langle T_{sp} \rangle$ derived from the spectrum integrals does not correspond to the temperature of any specific gas, since the averaging used above blends together all the gas on each line of sight. One way to interpret the mean spin temperature is to assume that the gas has two allowed temperatures, a cool phase at $T_c = 60$ K which causes all the absorption, and contributes by its column density, N_{cool}, to the emission, and a warm phase with column density N_{warm}, at some high temperature so that its absorption coefficient is negligible (several hundred degrees is enough, but physically this is likely to be about 6000 K). With this assumption the $\langle T_{sp} \rangle$ values translate into f_c, the mass fraction of cool gas, by

$$f_c = \frac{N_{cool}}{N_{warm} + N_{cool}} = \frac{T_c \tau}{N_{tot}} = \frac{T_c}{\langle T_{sp} \rangle}$$

(see DB). These cool gas fractions are given in the last column of Table 3. Of course these fractions depend on the choice of T_c, which is hard to determine even for nearby clouds because there is always some warm gas associated with the cloud which blends with the cool gas seen in absorption. A particularly careful attempt to separate the warm and cool components in emission by Mebold et al. (1982) suggests that 60 K is a representative value for the Milky Way.

The spectrum integrals given in Table 3 are biased slightly in favor of cool gas because of the threshold of 5 K in brightness temperature. Fainter emission typically comes from warmer

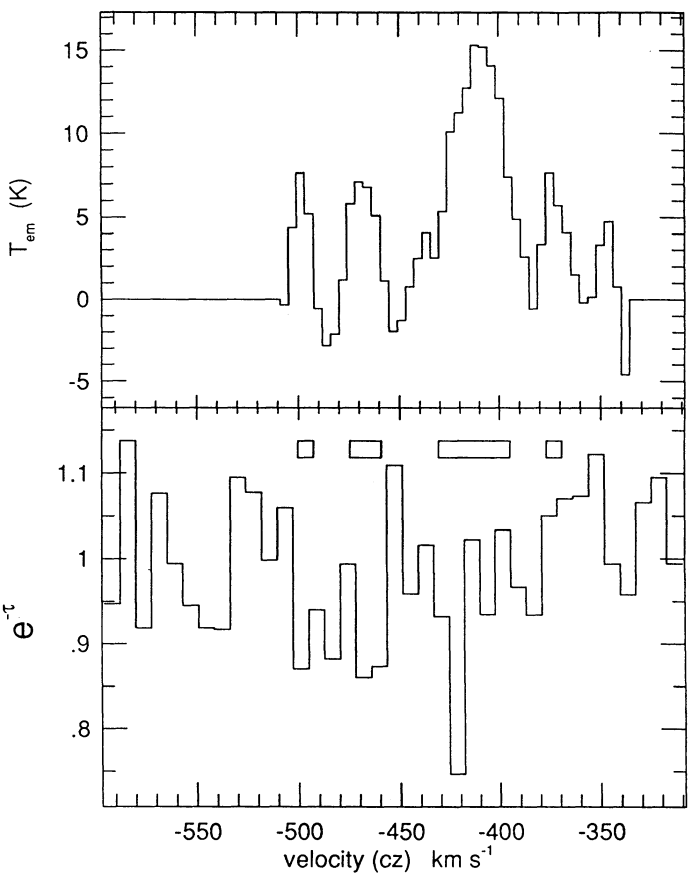

FIG. 4.—Spectra toward 37W052 in M31, presented as in Fig. 1

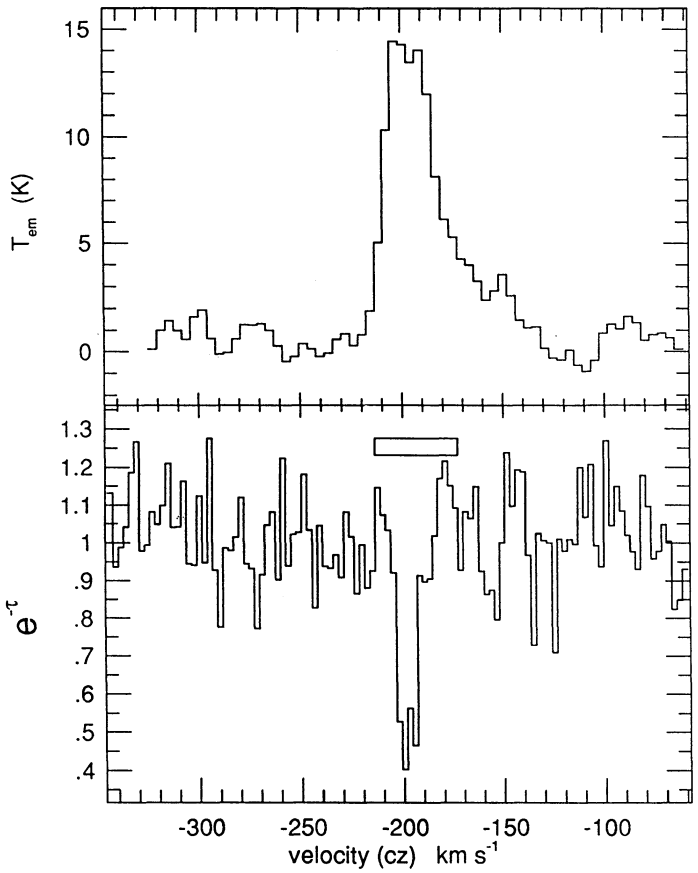

FIG. 5.—Spectra toward V11 in M33, presented as in Fig. 1

gas, and the brightness temperature of the emission can sometimes be an indication of its optical depth (Milky Way H I with brightness temperature above about 5 K often shows some absorption, as pointed out by Braun & Walterbos 1992.) Lowering the brightness threshold by a factor of 2 lowers the fraction of cool gas by about 30%.

4. DISCUSSION

In Table 4 the overall results of the project are compared with preceding work on the mixture of phases in spiral galaxies. The Milky Way data are summarized by Kulkarni (1984). The emission integrals are computed from the Bell Laboratories and Hat Creek surveys; the absorption integrals are averaged over surveys by Arecibo and Nançay. They are reduced to the effective half-thickness $|b| = 90°$ by weighting each observation by $\sin |b|$. The variation with $|b|$ of overall column densities reflects the relatively low abundance of atomic gas within about two scale heights ($\sim$300 pc) of the Sun, and particularly of cool atomic clouds, so that below $|b| = 30°$ both $\langle N \sin |b| \rangle$ and f_c increase. Results of preceding absorption surveys of M31 by DB and Braun & Walterbos (1992, hereafter BW) are listed in Table 4, also converted to effective disk half-thickness seen face-on, similar to $\langle N \sin |b| \rangle$ for the Milky Way data. This conversion includes multiplying the spectrum integral totals by $\cos |i|$, where i is the inclination, and dividing by twice the number of background sources. For M33 one continuum source is intrinsic (V106 = NGC 604), so we divide the absorption integral by 13 rather than 14, i.e., we assume that the line of sight sampled in absorption stops at midplane for V106. BW's survey covers a different area of M31, so that their data are independent of ours. The study of BD was hampered by low sensitivity in absorption, a small

TABLE 3

SPECTRUM INTEGRALS

A. M31

37W[a] (1)	$\int (1 - e^{-\tau}) dv$ (km s^{-1}) (2)	$\int T_{em}\, dv$ (K km s^{-1}) (3)	ΔV (km s^{-1}) (4)	$\langle T_{sp} \rangle$ (K) (5)	$f_c \equiv 60/\langle T_{sp} \rangle$ (6)
043	0.9 ± 1.7	220 ± 22	28.3	>43	...
045	1.2 ± 0.6	58 ± 9	5.1	>32	...
050	0.7 ± 0.9	290 ± 23	33.4	>107	<0.56
051	12.0 ± 1.8	650 ± 34	72.0	47–64	~1
052	4.2 ± 1.5	637 ± 33	66.9	112–236	0.25–0.54
057	1.0 ± 0.9	432 ± 23	33.4	>160	<0.38
067	2.3 ± 0.8	658 ± 30	54.0	212–439	0.14–0.28
081	13.1 ± 3.1	1495 ± 36	79.8	92–150	0.40–0.65
091	−0.3 ± 0.3	65 ± 9	5.1	>72	<0.83
Total	35.1 ± 4.5	4505 ± 78	378	112–150	0.40–0.54

B. M33

37W[a] (1)	$\int (1 - e^{-\tau}) dv$ (km s^{-1}) (2)	$\int T_{em}\, dv$ (K km s^{-1}) (3)	ΔV (km s^{-1}) (4)	$\langle T_{sp} \rangle$ (K) (5)	$f_c \equiv 60/\langle T_{sp} \rangle$ (6)
V8	−0.8 ± 2.4	596 ± 24	36.0	>79	<0.8
V11	3.9 ± 1.2	424 ± 26	41.2	80–160	0.4–0.7
V27	−2.8 ± 1.2	268 ± 20	23.2	>75	<0.8
V32	1.8 ± 0.7	367 ± 22	28.3	80–180	0.15–0.4
V37	1.0 ± 0.9	195 ± 17	18.0	>70	<0.8
V39	2.4 ± 1.1	188 ± 17	18.0	50–150	0.4–1
V106	2.5 ± 2.8	984 ± 31	59.2	>117	<0.5
Total	8.0 ± 4.4	2850 ± 59	227.8	>230	<0.26

[a] See text.

TABLE 4

AVERAGE GALAXY INTEGRALS

Galaxy	$\langle N \sin \lvert b \rvert \rangle$ (K km s^{-1})	$\langle \Delta V \sin \lvert b \rvert \rangle$ (km s^{-1})	$\langle \kappa \rangle$ (km s^{-1} kpc^{-1})	$\langle T_{sp} \rangle$ (K)	f_c
Milky Way					
$\lvert b \rvert > 30°$	150	0.34	2.3	441	0.14
$10° < \lvert b \rvert < 30°$	180	0.72	4.8	250	0.24
M31 ($i = 77°$)					
This paper	56 ± 1	0.44 ± 0.06	2.9	127	0.47
Braun & Walterbos 1992	134	0.77	4.9	174	0.34
Dickey & Brinks 1988	127	0.32	2.1	397	0.15
M33 ($i = 55°$)					
This paper	117 ± 2	0.35 ± 0.19	2.3	366	0.16

number of background sources (5 versus 7 for BW and 9 in this work), and a restricted velocity coverage so that some absorption may have been missed. The results of this project confirm the finding of BW that 21 cm absorption is relatively common in M31, even more than in the Milky Way. Apparently M31 is richer in cool H I than the Milky Way, at least that area of the Milky Way sampled by lines of sight with $\lvert b \rvert > 10°$, i.e., within about 1 kpc of the Sun.

In contrast to M31, M33 appears to show less absorption than the Milky Way. The seven lines of sight sampled here show on average about as low a fraction of cool H I as the high-latitude Milky Way sample, much lower than M31 and the Milky Way average on a larger scale. It is risky to generalize from so few lines of sight, but the suggestion of the M33 result is that there is a progression of cool gas abundances with spiral type. The Sb galaxy (M31) has a larger fraction of its atomic gas in the cool phase ($f_c = 0.4 \pm 0.1$), the Sc galaxy (M33) has a smaller fraction cool ($f_c = 0.16 \pm 0.1$), and the Milky Way is in between ($f_c \cong 0.25$).

The mean absorption coefficient, $\langle \kappa \rangle$, listed in Table 4, column (4), is a measure of $n/\langle T_{sp} \rangle$ at midplane. It is given by the absorption integral, $\langle \Delta V \sin \lvert b \rvert \rangle = \langle \int (1 - e^{-\tau}) dv \times \sin \lvert b \rvert \rangle$, divided by the effective path length through the absorbing layer at $\lvert b \rvert = 90°$, which is about 150 pc for the Milky Way, and we adopt the same for M31 and M33, at least inside the regions of warp and flaring of the outer gas disk. Convenient units for $\langle \kappa \rangle$ are km s^{-1} kpc^{-1}, which converts to $n/\langle T_{sp} \rangle$ units according to 1 cm^{-3} K^{-1} = 1692 km s^{-1} kpc^{-1}, and similarly for density (n) the units of K km s^{-1} kpc^{-1} are convenient, for which 1 cm^{-3} = 1692 K km s^{-1} kpc^{-1}. Since the filling factor of the cool gas is very low (~5%), we keep in mind that the absorption coefficient, $\langle \kappa \rangle$, is an average taken over a large volume, but that inside a cool cloud the local absorption coefficient is much higher. In the Milky Way at the solar circle $\langle \kappa \rangle$ has the value 5 km s^{-1} kpc^{-1} over a wide range of longitudes in the first quadrant, so the intermediate-latitude value shown in Table 4 is typical (Garwood & Dickey 1988). M31 apparently has a value of $\langle \kappa \rangle$ similar to the Milky Way solar circle value. For M33 it is lower by about a factor of 2.

4.1. *The Peak Brightness Temperature*

A quantity more easily measured than the optical depth, which also relates to the mixture of phases in the atomic gas, is the peak brightness temperature of the 21 cm emission. In the Milky Way at low latitudes the 21 cm emission saturates at a value of 125 K (e.g., Burton 1971), which is independent of longitude as long as the line-of-sight velocity gradient is less than ~5 km s^{-1} kpc^{-1} (see the review by Burton 1988). This saturation is plainly the result of absorption by H I in the cool phase (Baker & Burton 1975). We would expect the Milky Way 21 cm emisson to saturate for those longitudes and velocities where $\langle \kappa \rangle$ is greater than the velocity gradient due to differential rotation, i.e., $\langle \kappa \rangle > dv/dr$, since for these places on the l-v diagram a line-of-sight length, Δr, corresponding to velocity width Δv, will intersect cool gas with optical depth integral $\int (1 - e^{-\tau}) dv > \Delta v$, meaning that the optical depth averaged over that velocity range is large. The maximum velocity gradient seen anywhere in the Milky Way is about 90 km s^{-1} kpc^{-1}, but typical inner galaxy values are about 5–10 km s^{-1} kpc^{-1} (reviewed by Burton 1988, 1992), which explains the partial saturation of the 21 cm emission at low latitudes, since this is similar to the value of $\langle \kappa \rangle$.

The peak T_B value of 125 K is easy to understand on the basis of the midplane values of the density of warm, optically thin gas and of $\langle \kappa \rangle$. The z-distribution of H I gas is somewhat complex, but there appears to be a component with scale height about 150 pc, which we tentatively identify with the cloud layer (both cool gas and warm gas associated with the clouds), plus a much broader component with scale height 300–500 pc. This broader component has a larger filling factor than the clouds have, even at midplane, somewhere in the range 10%–50%, and is mostly warm, optically thin H I. The peak brightness temperature must saturate at a value given by the spin temperature of the clouds, say 60–75 K, plus the brightness contributed by the warm phase along the line of sight in front of the first optically thick cloud (Fig. 6). The amount of this warm phase contribution depends on the mean density of warm gas (about 0.2 cm^{-3}, or 330 K km s^{-1} kpc^{-1}) and on the mean free path between clouds. Each of these may be a function of position, and so of velocity at low latitudes. Using a typical velocity width $\delta v \sim 5$ km s^{-1} (set by turbulence in the clouds) gives the mean free path:

$$\lambda_{\rm mfp} = \frac{\delta v}{\langle \kappa \rangle} .$$

So in the Milky Way disk at the solar circle the mean free path is roughly 1 kpc. The peak brightness temperature is just the cold cloud temperature plus the mean free path times the warm

gas density divided by the velocity width, i.e.,

$$T_{B\,\max} = T_c + \frac{n_w \lambda_{\rm mfp}}{\delta v} = T_c + \frac{n_w}{\langle \kappa \rangle} .$$

Milky Way values of $T_c \sim 60$ K, $n_w \cong 330$ K km s^{-1} kpc^{-1}, and $\langle \kappa \rangle \cong 5$ km s^{-1} kpc^{-1} give $T_{B\,\max} \cong 125$ K, as observed. Note that this is independent of the filling factor of either phase, and applies as long as the velocity gradient is less than $\langle \kappa \rangle$, which is the condition for saturation.

M31 is similar to the Milky Way in midplane density and overall scale height for the H I layer. Seen from inside the disk of M31, the 21 cm emission probably saturates at about 125 K as we see for the Milky Way. There is no evidence to suggest that the cloud temperature in M31 differs much from that in the Milky Way. However, looking into the disk from outside, we see a higher peak brightness temperature because of the "overburden" of warm gas at high z above the midplane (Fig. 6). In fact, the peak values for T_B measured by the VLA synthesis of Braun (1990a, b) are as a high as 180 K. This is what would be expected for the Milky Way also if it were viewed from outside at inclination angle 77° as we view M31. The reason for the higher brightness temperature is the long path at high z through warm, optically thin gas *before* hitting the layer of optically thick clouds near $z = 0$.

Warm gas dominates at high z fundamentally because the gas pressure is lower there. In the static model of FGH the cool phase can exist only for $P/k > \sim 300$ K cm^{-3} (depending on the cosmic-ray ionization rate and the metallicity, reviewed by Shull 1987), which translates to $z < \sim 220$ pc assuming $P/k = 3500 \exp(-z^2/2\sigma^2)$ K cm^{-3} with $\sigma = 100$ pc (see Lockman & Gehman 1991), where for simplicity we identify σ with the width of the cool H I layer (but see Kulkarni & Heiles 1988 for arguments that σ is as large as 400 pc). The FGH model is unrealistic in many ways, but this basic feature carries over to dynamic theories. In the MO model the fraction of cool phase H I decreases with z because of a lower rate of H I condensation onto cool clouds during the intervals between being engulfed by young supernova remnants (Wang & Cowie 1988). The Milky Way and M31 apparently have supernova rates which put them in the fountain or "chimney" mode of Norman & Ikeuchi (1989; see also Boulares & Cox 1990), as evidenced by the larger number of shells and supershells (Brinks & Bajaja 1986; Heiles 1979). This means that these galaxies are intermediate between having a hot wind which escapes altogether and an ordinary two-phase halo. In this context the high-z H I is still entirely in the warm phase, as it exists largely as fountain gas condensing from the warmer halo and falling back toward the plane.

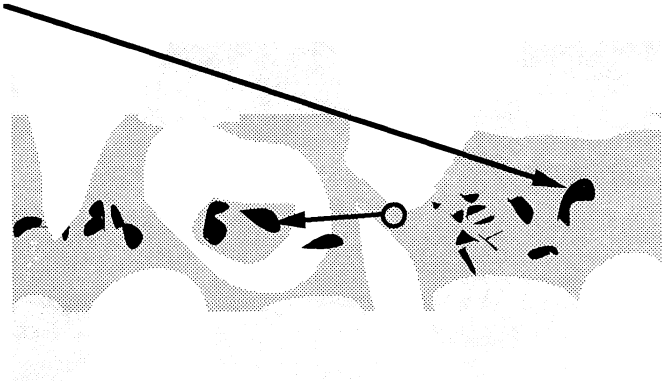

FIG. 6.—Schematic showing the geometry of saturation in the 21 cm line. The mean free path (which is a function of velocity at low latitudes) is determined by the abundance of cool, optically thick clouds. The peak brightness temperature is given by their brightness temperature plus the brightness temperature contributed by the warm gas in front of the first cloud. Seen from outside, there is an "overburden" of warm gas at high z which raises the peak brightness temperature above the value seen from inside the disk.

In the Milky Way there is direct observational evidence that the mean spin temperature increases with z (Kulkarni et al. 1984). We also know that the z-distribution of H I absorption is much narrower than that of the H I emission. The absorption, $\langle \kappa \rangle$, is distributed roughly as a Gaussian with scale height 150 pc (Dickey et al. 1981), whereas the total gas distribution shown by the emission includes another component, a broad exponential ("the Lockman layer") with scale height ~ 500 pc, which is apparently warm gas exclusively (Dickey & Lockman 1990; see also Lockman & Gehman 1991). So looking down into the Milky Way disk from above $|b| = 90°$, a line of sight would first traverse warm gas with column density $N \cong 10^{20}$ cm^{-2} = 56 K km s^{-1} before hitting the layer of cool clouds.

Looking into the Milky Way from outside along a line of sight with $|b| = 13°$, as we see M31, the vertical stratification of the warm and cool H I would have a very large effect on the 21 cm brightness temperature. The path length through the warm, high-z gas before hitting any clouds becomes very long at such high inclination. For the Milky Way a total warm gas column density of $N_{{\rm high}\,z} = 4.4 \times 10^{20}$ cm^{-2} = 240 K km s^{-1} would be collected above 150 pc, i.e., before hitting the cloud layer. So the peak brightness temperature is raised above the value it would have as seen from inside the disk by some $T_{\rm excess} = N_{{\rm high}\,z}/\delta v$. The value of $T_{\rm excess}$ depends on δv, which now includes contributions from differential rotation along the line of sight above 150 pc. For a typical value of $\delta v = 5$ km s^{-1} we can expect $T_{\rm excess} \cong 50$ K. Thus for M31 the peak brightness temperature seen from our point of view should be about 50 K + 125 K, roughly what is observed.

M33 is a very different case because it is much more face-on. Seen face-on, none of M31, M33, or the Milky Way is optically thick, on average, since, for all three, $\delta v/\langle \kappa \rangle$ is greater than the scale height of cool clouds. Thus only a few clouds will show high optical depth, and the beam filling factor of these will be small, just as the covering factor of optically thick gas seen at high latitudes in the Milky Way is small. The 21 cm line saturates only if the inclination is higher than $|\sin i| > \lambda_{\rm mfp}/(2\pi)^{1/2}\sigma$, with σ the scale height of the absorption layer. The peak brightness temperatures seen in M33 by Deul & van der Hulst (1987) are roughly 95 K, much less than for M31 or the Milky Way. Assuming the same stratification of the warm gas as in the Milky Way, we would expect the peak brightness temperature to be about 20–30 K above the temperature of the clouds themselves.

The importance of the gravitational potential shape in determining the mixture of warm and cool phases, and hence the peak brightness, is evident when comparing with the extreme case of dwarf irregular galaxies. In this case the gravitational potential is evidently much more shallow than in the Milky Way disk, so that there is a large halo of atomic hydrogen at low pressure where the cool phase cannot exist in thermal equilibrium. Evidence for these extended halos comes from the immense shells and supershells seen in dwarfs by Puche et al. (1992); the scale height of the gas must be at least as large as the largest supershells, which can be as big as a kiloparsec. In this case the peak brightness temperatures can be very high, since the line of sight through the warm layer is very long before entering the relatively small region where the cool, opti-

cally thick clouds can exist. Brightness temperatures in excess of 200 K are sometimes observed in these systems.

5. CONCLUSIONS

The main conclusion from this work is that the warm neutral medium is robust. It is the dominant form of the atomic hydrogen in M31 and M33, as it is in the Milky Way. These galaxies differ in many ways from the Milky Way, in heavy-element abundances which control the cooling rate, in star formation rates, and in molecular gas fraction, yet still they show a mixture of warm and cool phase atomic gas remarkably similar to that in the solar neighborhood. Although not many absorption lines are detected in this survey, the amount of absorption detected in M31 is slightly larger than would be expected from the Milky Way, indicating that the abundance of cool phase H I is somewhat greater than for the solar neighborhood. In M33 there is considerably less absorption detected than would be expected (given the emission in the directions of the background sources), so the fraction of gas in the warm phase must be higher than in M31 or the Milky Way, at least 80%. It is possible that this represents a sequence in mixtures of thermal phases with Hubble type, as discussed in § 4 above.

It is possible that the temperature of the cloud phase is different in these galaxies, as suggested by BW for M31. However, we do not see any differences in the properties of the 21 cm emission or absorption which would necessitate this hypothesis. The striking difference in the peak brightness temperature of the 21 cm emission we interpret as a natural result of the thermal stratification of the disk, and the difference in our vantage points for M31 and for the Milky Way disk. The relationships between mean pressure, supernova rate, gravitational potential shape, and coolant abundance suggest that dwarf irregular galaxies should show an even larger fraction of warm phase H I, as seems to be the case in Ho 2. Surveys of 21 cm absorption through the Magellanic Clouds, such as that of Mebold et al. (1991), will further test this idea.

We are grateful to Jacqueline van Gorkom, Evan Skillman, Ed Salpeter, Neb Duric, Rob Kennicutt, Robert Braun, Rene Walterbos, Barry Clark, Miller Goss, Jay Lockman, Baerbel Koribalski, Butler Burton, Carl Heiles, Doug Wood, Dale Frail, and many others for useful conversations. This research was supported in part by NSF grant 87-22990 to the University of Minnesota.

REFERENCES

Baker, P. L., & Burton, W. B. 1975, ApJ, 198, 281
Boulares, A., & Cox, D. P. 1990, ApJ, 365, 544
Braun, R. 1990a, ApJS, 72, 755
———. 1990b, ApJS, 72, 761
Braun, R., & Walterbos, R. 1992, ApJ, 386, 120 (BW)
Brinks, E., & Bajaja, E. 1986, A&A, 169, 14
Brinks, E., & Shane, W. W. 1984, A&AS, 55, 179
Burton, W. B. 1971, A&A, 10, 76
———. 1988, in Galactic and Extragalactic Radio Astronomy, ed. G. L. Verschuur & K. Kellermann (New York: Springer-Verlag), 295
———. 1992, Saas-Fée Lecture Notes (Berlin: Springer-Verlag), in press
Clark, B. G. 1965, ApJ, 142, 1398
Cowie, L. L. 1987, in Interstellar Processes, eds. D. J. Hollenbach & H. A. Thronson, Jr. (Dordrecht: Reidel) p. 245
Cox, D. P. 1990, in The Interstellar Medium in Galaxies, ed. H. A. Thronson & J. M. Shull (Dordrecht: Kluwer), 181
Cox, D. P., & McCammon, D. 1986, ApJ, 304, 657
Deul, E. R., & van der Hulst, J. M. 1987, A&AS, 67, 509
Dickey, J. M., & Brinks, E. 1988, MNRAS, 233, 781 (DB)
Dickey, J. M., Brinks, E., & Puche, D. 1992, ApJ, 385, 501
Dickey, J. M., & Lockman, F. J. 1990, ARA&A, 28, 215
Dickey, J. M., Weisberg, J. M., Rankin, J. M., & Boriakoff, V. 1981, A&A, 101, 332
Field, G. B., Goldsmith, D. W., & Habing, H. J. 1969, ApJ, 155, L149 (FGH)
Frail, D. A., Cordes, J. M., Hankins, T. H., & Weisberg, J. M. 1991, ApJ, 382, 168
Garwood, R. W., & Dickey, J. M. 1988, ApJ, 338, 841
Heiles, C. 1979, ApJ, 229, 533
———. 1990, ApJ, 354, 483
Hunter, D. A., & Gallagher, J. S., III. 1990, ApJ, 362, 480
Kobulnicky, H., Dickey, J. M., & Garwood, R. W. 1993, in preparation
Kulkarni, S. R. 1984, Ph.D. thesis, Univ. California at Berkeley
Kulkarni, S. R., & Heiles, C. 1987, in Interstellar Processes, ed. D. J. Hollenbach & H. A. Thronson, Jr. (Dordrecht: Reidel), 87
———. 1988, in Galactic and Extragalactic Radio Astronomy, ed. G. L. Verschuur & K. I. Kellermann (New York: Springer-Verlag), 95
Kulkarni, S. R., Heiles, C., van Gorkom, J., & Dickey, J. M. 1984, in IAU Colloq. 81, Local Interstellar Medium, ed. Y. Kondo, F. C. Bruhweiler, & B. D. Savage (NASA CP-2345), 269
Lockman, F. J., & Gehman, C. S. 1991, ApJ, 382, 182
McKee, C. F., & Ostriker, J. P. 1977, ApJ, 218, 148 (MO)
Mebold, U., Winnberg, A., Kalberla, P. M. W., & Goss, W. M. 1982, A&A, 115, 223
Mebold, U., et al. 1991, A&A, 251, L1
Norman, C. A., & Ikeuchi, S. 1989, ApJ, 245, 372
Payne, H. E., Salpeter, E. E., & Terzian, Y. 1983, ApJ, 272, 540
Puche, D., Brinks, E., Westphal, D., & Roy, I. R. 1992, AJ, in press
Rand, R. J., Kulkarni, S. R., & Hester, J. J. 1990, ApJ, 352, L1
Shaya, E. J., & Federman, S. R. 1987, ApJ, 319, 76
Shull, J. M. 1987, in Interstellar Processes, ed. D. J. Hollenbach & H. A. Thronson, Jr. (Dordrecht: Reidel), 225
Tilanus, R. P. J., & Allen, R. J. 1989, ApJ, 339, L57
Viallefond, F., Goss, W. M., van der Hulst, J. M., & Crane, P. C. 1986, A&AS, 64, 237
Walterbos, R. A. M., Brinks, E., & Shane, W. W. 1985, A&AS, 61, 451
Wang, Z., & Cowie, L. L. 1988, ApJ, 335, 168
Wyse, R. F. G. 1986, ApJ, 311, L41